Molybdate inhibits mercury methylation capacity of Pseudodesulfovibrio hydrargyri BerOc1 regardless of the growth metabolism

Diva Scuvée, Marisol Goñi, Emmanuel Tessier, Claire Gassie, Magali Ranchou-Peyruse, David Amouroux, Remy Guyoneaud, Bahia Khalfaoui-Hassani

Molybdate inhibits mercury methylation capacity of *Pseudodesulfovibrio hydrargyri* BerOc1 regardless of the growth metabolism

Diva Scuvée[1], Marisol Goñi-Urriza[1], Emmanuel Tessier[1], Claire Gassie[1], Magali Ranchou-Peyruse[2], David Amouroux[1], Rémy Guyoneaud[1] and Bahia Khalfaoui-Hassani[1]*

[1]Université de Pau et des Pays de l'Adour, E2S UPPA, CNRS, IPREM, Pau, France
[2]Université de Pau et des Pays de l'Adour, E2S UPPA, CNRS, LaTEP, Pau, France

[*]**Corresponding Author:** Bahia Khalfaoui-Hassani, b.khalfaoui-hassani@univ-pau.fr

Abbreviations: sulfate-reducing bacteria, SRB; mercury, Hg; inorganic mercury, Hg(II); monomethylmercury, MeHg; sulfate adenylyltransferase, Sat enzyme; adenosine 5'-phosphosulfate, APS; Ct: Cycle threshold.

Abstract

Molybdate inhibits sulfate respiration in sulfate-reducing bacteria (SRB). It is used as inhibitor to indirectly evaluate the role of SRB in mercury methylation in the environment. Here, the SRB *Pseudodesulfovibrio hydrargyri* BerOc1 was used to assess the effect of molybdate on cell growth and mercury methylation under various metabolic conditions. *Geobacter sulfurreducens* PCA was used the non-SRB counterpart strain with the ability to methylate mercury. While PCA growth and methylation are not affected by molybdate, 1 mM of molybdate inhibits BerOc1 growth under sulfate respiration (50% inhibition) but also under fumarate respiration (complete inhibition). Even more surprising, mercury methylation of BerOc1 is totally inhibited at 0.1 mM of molybdate when grown under sulfate or fumarate respiration with pyruvate as electron donor. As molybdate is expected to reduce cellular ATP level, the lower Hg methylation observed with pyruvate could be the consequence of lower energy production. Although molybdate alters the expression of *hgcA* (mercury methylation marker) and *sat* (involved in sulfate reduction and molybdate sensitivity) in a metabolism-dependent manner, no relationship with mercury methylation rates could be found. Our results show, for the first time, a specific mercury methylation inhibition by molybdate in SRB.

Keywords: Sulfate respiration; fumarate respiration; sulfate-reducing bacteria; methylmercury methylation; molybdate inhibition; mercury methylation.

Introduction

Mercury (Hg) is a toxic metallic element that poses significant environmental and public health concerns. While all forms of mercury are considered hazardous, methylated forms, such as monomethylmercury (MeHg), are the most alarming (Hong Young-Seoub, 2012). MeHg is neurotoxic, primarily produced by microorganisms. This organic form of Hg is bio-accumulated and bio-amplified in food webs putting at risk humans and wildlife (Chen et al., 2008; Ma et al., 2019). The predicted membrane-attached methyltransferase HgcA and the ferrodoxin-like protein HgcB are so far the only identified proteins implicated in the transformation of inorganic mercury Hg(II) into MeHg (Cooper et al., 2020; Parks et al., 2013; Smith et al., 2015). HgcA is thought to transfer the methyl group to Hg(II) via its corrinoid cofactor, while HgcB acts as an electron donor via its Fe-S cluster to re-activate the catalytic cycle. *hgcAB* cluster is currently used as a bioindicator of Hg methylation in a large number of ecological studies (e.g., Bouchet et al., 2018; Podar et al., 2015; Vigneron et al., 2021; Villar et al., 2020).

Hg methylation process is associated with the activity of iron reducing bacteria and methanogens (Bravo et al., 2018; Gilmour et al., 2018), along with the activity of sulfate reducing bacteria (SRB). The Hg methylation activity of the SRB group has been extensively studied (e.g., Gilmour et al., 1992; Goñi-Urriza et al., 2020; King et al., 2000; Ranchou-Peyruse et al., 2009). The SRB belongs to the group of sulfate reducing prokaryotes capable of utilizing sulfate as terminal electron acceptor in order to perform the dissimilatory reduction of sulfate to sulfide (Barton and Fauque, 2009), the so called sulfate respiration. The sulfate respiration is initiated by the ATP-dependent activation of sulfate via the sulfate adenylyltransferase (ATP sulfurylase or Sat enzyme), to generate adenosine 5'-phosphosulfate (APS) and inorganic pyrophosphate (Keller and Wall, 2011). After the activation, APS is reduced to bisulfite with the APS reductase AprBA (Meyer and Kuever, 2008). The produced bisulfite is further reduced to (bi)sulfide by the dissimilatory (bi)sulfite reductase DsrAB (Ferreira et al., 2022; Oliveira et al., 2008).

Oxyanion analogs of sulfate, such as molybdate (MoO_4^{2-}), tungstate, selenate, chromate, arsenate, etc, are selective inhibitors of sulfate reduction activity (Carlson et al., 2021; Taylor and Oremland, 1979). Molybdate, for instance, has been widely used as a specific inhibitor of sulfate respiration in different physiological (e.g., Biswas et al., 2009; Tucker et al., 1997) and ecological studies (e.g., Bouchet et al., 2018; Kleikemper et al., 2002; Lee et al., 2014). Studies on selected SRB strains suggested that the effect of molybdate is partially due to the inhibition of cellular sulfate transport (Newport and Nedwell, 1988). However, since molybdate did not affect sulfate accumulation (Cypionka, 1989), it is unclear whether molybdate inhibits sulfate transport. The inhibition of the sulfate-respiring organisms by molybdate, and other oxyanions of the group VI elements, is also thought to be

linked to an intracellular decrease of ATP level (Taylor and Oremland, 1979). The Sat enzyme is thought to be one of the targets in this inhibition, since Sat catalyzes in the presence of molybdate the formation of an unstable APS analog (adenosine 5'-molybdophosphate), leading to a fast ATP hydrolysis and a non-productive ATP cycling. However, a Δ*sat* mutant of *Desulfovibrio vulgaris* Hildenborough remained sensitive to molybdate (Zane et al., 2020). Notwithstanding, strain lacking both Sat and a newly identified YcaO-like protein become resistant to molybdate (Zane et al., 2020). Although the mode of action of YcaO-like protein in the SRB-inhibition by molybdate remains unknown, the authors hypothesized that it is similar to that of the Sat enzyme (Zane et al., 2020).

The inhibition of the sulfate reduction by molybdate is widely used to evaluate the ecological role of SRB in the Hg methylation process in ecosystems (e.g., Bouchet et al., 2018; Fleming et al., 2006; Gentès et al., 2013; Hines et al., 2012). However, SRB are metabolically versatile, and may shift from one metabolism to other in the presence of molybdate, in order for microorganisms to remain active. Interestingly, previous study conducted by our group in the Lake Titicaca hydrosystem (Bolivian Altiplano) showed that sulfate reducers were still active in biofilm and periphyton upon the addition of molybdate, while the Hg methylation process was inhibited by more than 90% (Bouchet et al., 2018). The sulfate reducers remained active in the presence of molybdate, probably because they switched from sulfate respiration to another growth metabolism, as suggested by the observed absence of H_2S production (Bouchet et al., 2018). The effect of molybdate on Hg methylation in this study is perplexing, especially considering that Hg methylation potential in SRBs has been found to be higher under non-sulfidogenic growth conditions than under sulfidogenic growth conditions in cell culture studies (Barrouilhet et al., 2022; Compeau and Bartha, 1985) as well as in ecological studies (Compeau Geoffrey C. and Bartha Richard, 1987; Gilmour and Henry, 1991). Indeed, under non-sulfidogenic growth, Hg is expected to be more bioavailable for methylation (Benoit J. M. et al., 2001; Benoit et al., 2001). Moreover, molybdate can be complexed to sulfides in a sulfide-rich environment (i.e. sulfate respiration) (Biswas et al., 2009; Tucker et al., 1997). Consequently, the rate of mercury methylation may vary depending on whether molybdate is utilized under sulfidogenic growth conditions as opposed to non-sulfidogenic growth conditions, such as fumarate respiration. The molybdate-induced inhibition of Hg methylation in a microbial community where sulfate reducers are still active (Bouchet et al., 2018) is not fully understood. In such a complex structure, it is certainly difficult to tease apart the mode of action of molybdate, especially whether it directly or indirectly affects the growth mode of SRB or their Hg methylating activities. Likewise, molybdate induced-inhibition of Hg methylation of non-sulfate reducers in such a complex environment is difficult to decipher.

In this work, the SRB and the Hg methylating model bacterium, *Pseudodesulfovibrio hydrargyri* BerOc1 was used, to assess the impact of molybdate on cell growth and the Hg methylation process in three different growth conditions, including sulfidogenic growth conditions (two under sulfate respiration) and non-sulfidogenic growth (fumarate respiration). To further understand the mechanisms of molybdate inhibition, the expression level of *hgcA* gene involved in Hg methylation (Parks et al., 2013), *sat* and *ycaO* genes involved in molybdate-sensitivity (Zane et al., 2020) were investigated when molybdate inhibition was induced. Additionally, the Non-SRB and the iron-reducer *Geobacter sulfurreducens* PCA, which is also capable of Hg methylation, was employed to evaluate whether the specific effect of molybdate on Hg methylation could be extended to non-SRB strains.

Experimental procedures

Strains and culture conditions

Two Hg-methylating strains were used in this study; the sulfate reducing bacterium *P. hydrargyri* BerOc1 (Ranchou-Peyruse et al., 2018) and the iron reducing bacterium, *G. sulfurreducens* PCA (Lin et al., 2014). *P. hydrargyri* BerOc1 is a model organism for studying the mechanisms of mercury methylation at the cell level (Bakour et al., 2023; Barrouilhet et al., 2022; Goñi-Urriza et al., 2015; Isaure et al., 2020). This bacterium can use lactate and pyruvate as electron donor for sulfate respiration (Ranchou-Peyruse et al., 2018) and pyruvate as electron donor for fumarate respiration (Barrouilhet et al., 2022). *G. sulfurreducens* PCA is capable of using acetate as electron donor in fumarate respiration (Caccavo F et al., 1994). Strains were cultivated under anoxic conditions in a common minimal medium (adapted from DSMZ), supplemented with different substrates in respect to their growth conditions. The medium contained the following (in $g.L^{-1}$, unless otherwise indicated): NH_4Cl, 0.25; NaCl, 10; KH_2PO_4, 0.2; $MgSO_4$, 0.4; $MgCl_2$, 0.4; $CaCl_2.2H_2O$, 0.1; KCl, 0.5; Hepes, 10 mM; trace element SL12 (1 $mL.L^{-1}$; composed of (in $g.L^{-1}$): H_3BO_3, 0.3; $FeSO_4.7H_2O$, 1.1; $CoCl_2.6H_2O$, 0.19; $MnCl_2.2H2O$, 0.05; $ZnCl_2$, 0.042; $NiCl_2.6H_2O$, 0.024; $Na_2MoO_4.2H_2O$, 0.018; and $CuCl_2,.2H_2O$, 0.002 (modified from (Overmann et al., 1992)), and 1 $mL.L^{-1}$ selenite/tungstate solution (composed of NaOH, 0.5 g; Na_2SeO_3, 2 mg and $Na_2WO_4.2H_2O$, 4 mg for 1 liter of water at pH 7.0). After autoclaving, the culture media were flushed with N_2 gas and supplemented with 1 $ml.L^{-1}$ of filtered V7 vitamin solution (Pfennig and Trüper, 1992) containing (in $mg.L^{-1}$) biotin, 2; para-aminobenzoate, 10; thiamin, 10; pantothenate, 5; pyridoxamin, 50; cobalamin, 20 and nicotinate, 20. *P. hydrargyri* BerOc1 was grown at 37°C on either sulfate or fumarate respiration. For the sulfate reducing growth condition, the medium was supplemented with either Na-sulfate (40 mM) and Na-pyruvate (40 mM) or with Na-sulfate (40 mM) and Na-lactate (40 mM) as substrates. For the fumarate respiration condition, the medium was supplemented

with Na-fumarate (40 mM) and Na-pyruvate (40 mM). *G. sulfurreducens* PCA was grown at 30°C on fumarate respiration in medium supplemented with Na-acetate (10 mM) and Na-fumarate (50 mM) as substrates.

For all experiments described below, the strains were cultivated for 24h in sulfate respiration and 48h in fumarate respiration. Once grown, the cultures were opened in the anaerobic chamber and diluted two times by adding fresh culture medium and spiked with 0.05 µM of Hg(II) (from $HgCl_2$) or 0.0047 µM of MeHg (from CH_3HgCl). As shown previously, no toxic effect was observed for *P. hydrargyri* BerOc1 (Isaure et al., 2020) and PCA (Wang et al., 2013) at these Hg concentrations. Then, 10 ml of culture were distributed in 10 ml Bellco tubes containing the appropriate concentrations of molybdate ($Na\text{-}MoO_4$) (ranging from 0 to 2 mM for *P.hydragyri* BerOc1 and from 0 to 10 mM for *G. sulfurreducens* PCA) and were sealed with Teflon stoppers. Cells were collected for initial time measurements (T0) and stored until analysis, as described below. Then, tubes were incubated for 10h for *P. hydrargyri* BerOc1 in sulfate reducing conditions and 24h in fumarate respiration for both *P. hydrargyri* BerOc1 and *G. sulfurreducens* PCA. Cell growth was monitored following optical density (OD) at 600 nm until the end of the growth. Experiments were performed in triplicates. For each molybdate concentration, a control was performed without $HgCl_2$. At the end of the experiments, tubes were homogenized and samples were collected for final time measurements (Tf) and stored for each analysis (MeHg and Hg(II) production, quantification of cell number, metabolite productions and gene expressions), as described below.

Quantification of bacterial cell numbers

The cell numbers in each culture were determined by flow cytometry. Briefly, 40 µl of filtered formaldehyde (38%) were added to 800 µl of cultures at T0 and Tf, and stored at -80°C, until needed. Defrosted samples were labelled with Sybr Green 10X (Invitrogen) in a dark incubation during 15 min, and counted using Trucounts beads (BD), then injected in the cytometer (BD Accuri C6 cytometer, TBMCore) with Trucounts beads (BD) as internal standard. The minimal medium used was also injected in the cytometer to determine background noises and subtract it from the sample measurements.

Measurement of MeHg and Hg(II) productions

Similar methods were performed to measure MeHg/Hg(II) production. To measure either the MeHg or Hg(II) produced in the samples, 500 µl of cell culture from each sample were collected and added to 500 µl of nitric acid 6N at T0 and Tf. The MeHg/Hg(II) produced was detected using gas chromatography coupled to inductively plasma mass spectrometry (GC-ICP-MS) (Monperrus et al., 2008). A derivatization of the samples was performed to produce species of volatile ethylated Hg, easily separated via gas chromatography. Samples were then

transferred into vials containing 5 ml of water and 5 ml of acetic acid/acetate 0.1 M pH 3.9 buffer. Species specific isotope dilution analysis was used to accurately quantify Hg(II) and MeHg in culture medium. To this end, appropriate concentrations of Hg isotopes (^{199}HgII and ^{201}MeHg) were added to obtain an isotopic ratio close to 1 and the pH was adjusted between 3.85 and 4.05. After adjusting the pH, 500 µl of isooctane and 80 µl of tetraethylborate were added and samples were subjected to constant shaking for 20 min. The organic phase was collected and injected in the GC-ICP-MS. Chromatograms obtained were treated with the software PlasmaLab. To calculate the MeHg/Hg(II) produced by strains, MeHg/Hg(II) concentrations measured at the initial time were subtracted from the concentrations obtained at the final time. The detection limit of Hg compounds for GC-ICP-MS analytical method were 0.01 ng/g and 0.042 ng/g for iHg and MeHg, respectively. In all the tested conditions, the average concentration of MeHg found at the end of the incubations in the controls without Hg(II) were 0.05 +/- 0.01 ng/g. The percentage of recovery of mercury species was 75.08% +/- 10.86% in average.

Measurement of electron donors/acceptors and their produced metabolites

The consumption of electron donor and acceptor and the metabolite produced during the growth of *P. hydrargyri* BerOc1 grown in the presence of 0, 0.01 and 0.1 mM of molybdate, were analyzed using ion chromatography. Calibration curve was performed with sulfate, pyruvate, lactate, fumarate, acetate and succinate at concentration values of 0, 2, 4, 6, and 10 mg/L. 500 µl of cell culture from each sample were collected at T0 and Tf, filtered using syringe filters IC Millex® (0.20 µm) and stored at 4°C, until analysis. Samples were diluted 1000 times to obtain a salt concentration of 10 mg.L^{-1}. The liquid phase was analyzed on a Dionex ICS-1100 ion chromatography (ThermoFisher Scientific) equipped with a column Dionex ionpac AS11 HC with a pre-column Dionex AG11-HC used to remove metal contamination from samples and a DS6 heated conductivity detector (ThermoFisher Scientific). 125 µl of samples were injected. KOH was the eluent used with a gradient from 1 mM to 30 mM during the passage of the sample. Chromeleon program was used to analyze the data.

For sulfides quantification, 100 µl of cell cultures from each sample were added to 400 µl of 2% zinc acetate at T0 and Tf to trap the sulfides produced. Sulfide concentrations were quantified by a colorimetric method as describe by Cline (CLINE, 1969). A standard curve was carried out with a sulfide solution, and along with the samples, were quantified by the addition of 150 µl of DMPD (N,N-dimethylparaphenylenediamine sulfate) at 0.2% (m/v) and 10 µl of iron chloride at 10% (m/v). Samples were incubated 20 min at room temperature in the dark. The absorbance was measured at 670 nm in a microplate reader (Synergy HTX multi-mode reader (BioTek).

Quantification of gene expression level by qRT-PCR

To study the impact of molybdate on the expression of *hgcA*, *sat* and *ycaO* genes, *P. hydrargyri* BerOc1 strain was grown as described above, then the cell cultures (grown as previously described) were exposed to 100 ppb of HgII and different concentrations of molybdate (0, 0.01 and 0.1 mM). After 1h, the OD_{600} was measured and 5 ml of culture were collected. RNA protect (sodium acetate-saturated phenol: acetate (1M) pH 5.5 in 5% of saturated phenol and 95% ethanol) was added to each sample (at 0.6 of OD_{600}) at 1.25:10 ratio. Samples were vortexed and incubated 5 min at room temperature, then centrifuged 10 min at 8000 g at 4°C. Pellets were stored at -80°C, until RNA extraction. RNA extractions were performed using EXTRACT-ALL® Kit (Eurobio) according to the kit protocol guidelines. DNA contaminations were removed using TURBO DNase RNase-free™ Kit (Ambion). Purified RNA was quantified with Quant-iT RNA Assay Kit (Invitrogen™). RNA was diluted to obtain a concentration of 20 $ng.\mu l^{-1}$. cDNA was synthesized using M-MLV-RT (Invitrogen). Expression of *hgcA*, *sat* and *ycaO* genes, were quantified by quantitative Reverse-transcription PCR (qRT-PCR) in a CFX Connect Real-Time PCR Detection System using the DyNAmo™ ColorFlash SYBR® Green qPCR Kit (Finnzyme). 1 µl of cDNA was added with the appropriate primers in a final volume of 20 µl at 0.1 µM for *sat* and *ycaO* and 0.4 µM for *hgcA*. Primers used 1) for *hcgA* gene were peg.1401(hgcA)_DNDF1 (GTGCGGCTTCAAAGTGATCT) and peg.1401(hgcA)_DNDR1 (GAATATCTCCACCGGGATGA), 2) for *sat* gene were BerOc1_sat_F (CTACTGCTACAAGTGCGACG) and BerOc1_sat_R (TGCATCTTGACCTCGACCTT) and 3) for *ycaO* gene, were BerOc1_YcaO_F (AAGGATTTCTCGCTGGGCTA) and BerOc1_YcaO_R (TCTGGTCAAGCTCGGTGAAT). The housekeeping gene *gyrB* was used for normalization (Goñi-Urriza et al., 2015) with gyrBF1 (CCTCGAAGAAGGTGTTCAGC) and gyrBR1 (CCAAGAAGCTGGTCCAGAAG) primers. Real time PCR was carried out with an initial denaturation of 7 min at 95°C, followed by 45 cycles of 10 sec at 95°C, and 20 sec at 60 °C. Double delta Ct (Cycle Threshold) procedure using *gyrB* expression as reference was used to determine gene's induction level. PCR efficiency using each primer's pairs varied between 97% and 104%.

Statistical analysis

The non-parametric Kruskal-Wallis test and the Dunn test for pairwise comparisons were performed using R software.

Results

Effects of molybdate on the growth of P. hydrargyri *BerOc1 and* G. sulfurreducens *PCA*

The effect of molybdate on cell growth was evaluated in the sulfate-reducing bacterium, the SRB *P. hydrargyri* BerOc1, which is capable of Hg methylation (Ranchou-Peyruse et al., 2018). The non-sulfate reducing bacterium, *G. sulfurreducens* PCA, which is also capable of Hg methylation (Lin et al., 2014), was used to evaluate the effect of molybdate in a non-SRB strain (Fig. 1, Table 1 and Table S1). *P. hydrargyri* BerOc1 was grown in sulfate reducing metabolism in the presence of i) sulfate and pyruvate or ii) sulfate and lactate as substrates or in fumarate respiration with iii) fumarate and pyruvate as substrates. *G. sulfurreducens* PCA was grown in fumarate respiration in the presence of fumarate and acetate as substrates. As shown in Figure 1, 0.01 mM of molybdate has almost no effect on the biomass production of *P. hydrargyri* BerOc1 in all the tested conditions (Kruskal-Wallis test, $p > 0.05$). However, starting from 0.05 mM of molybdate, the biomass production of this bacterium decreases with the increase of molybdate concentrations in sulfate respiration as well as in fumarate respiration. Surprisingly, the biomass production of *P. hydrargyri* BerOc1 is reduced to less than 50% at 0.1 mM molybdate, as compared to 0 mM, in fumarate respiration (Fig. 1, inset). The growth is then completely inhibited at 1 mM in fumarate respiration (Dunn test $p = 0.0135$), while complete inhibition of biomass production is observed in sulfate-reducing metabolisms at 2 mM. The differences are statistically significant compared to 0 mM molybdate for both lactate and pyruvate as electron donors ($p<0.05$, Kruskal-Wallis test). For all the concentrations tested, molybdate has no impact on the biomass production of *G. sulfurreducens* PCA (Fig. 1), nor on the growth rate, even up to 10 mM (Table S1).

Molybdate inhibits Hg(II) methylation in P. hydrargyri *BerOc1*

The Hg methylating capacity of *P. hydrargyri* BerOc1 and *G. sulfurreducens* PCA, was evaluated in the presence of molybdate. The MeHg production was reported in ng of MeHg produced/cell (Fig. 2 and table S2). Interestingly, Hg(II) methylation is inhibited in the SRB *P. hydrargyri* BerOc1 grown in some of the tested conditions upon addition of molybdate, with a more pronounced difference at 0.05 mM of molybdate ($p<0.05$, Kruskal-Wallis test). Although the cell growth is still observed at 0.1 mM of molybdate in fumarate respiration (Fig.1 inset), the production of MeHg is completely inhibited at this concentration (Fig. 2, inset). Similar results are observed for *P. hydrargyri* BerOc1 cells grown in sulfate respiration in the presence of pyruvate as electron donor. The production of MeHg is much less inhibited by molybdate under the sulfate-reducing condition with lactate as the electron donor (Fig. 2). However, the molybdate-inhibition in the latter condition becomes complete when molybdate concentration reaches 2 mM, a concentration at which no bacterial growth is observed. For the iron-reducing bacterium *G. sulfurreducens*, molybdate does not affect the production of MeHg even up to 10 mM of molybdate (Fig. 2, table S2). The MeHg produced/cell represents the mean of all cellular states and account for

the viable as well as the non-viable cells, that can partially exist across all the growth conditions. The rate of MeHg production have been calculated and showed the same trends as the MeHg produced/cell (Table S2).

To investigate whether molybdate inhibition of MeHg production is directly due to a decrease of Hg(II) methylation or indirectly due to an increase of MeHg demethylation, the impact of molybdate on MeHg demethylation was also investigated in *P. hydrargyri* BerOc1 (Table S2). Similarly to the MeHg production experiments, the production of Hg(II) was quantified after the exposition of the cells to increasing molybdate concentrations as well as to 0.0047 µM of MeHg (not toxic for *P. hydrargyri* BerOc1 (Isaure et al., 2020)). No relationship between molybdate concentration and MeHg demethylation could be found (Table S2). These results showed that molybdate inhibition of Hg(II) methylation in *P. hydrargyri* BerOc1 is not due to an increase of the cellular MeHg demethylation.

Effect of molybdate on the consumed substrates and the produced metabolites

As described above, molybdate inhibits the growth and the Hg methylation activity of *P. hydrargyri* BerOc1 in all the tested metabolisms, although the rates of the inhibition vary. To ensure that the growth of *P. hydrargyri* BerOc1 in the presence of molybdate corresponds to the initially tested metabolism and is not due to a cellular metabolism circumvention (caused by a switch of the growth to other metabolisms (*e.g.* fermentation)), the concentrations of the provided substrates (electron donors and acceptors) and the expected produced metabolites of each condition were separated and quantified at the final time of the growth (Tf) (Table 1, Fig. 3). Metabolites were only measured in conditions where molybdate does not affect (or only slightly affect) the growth of *P. hydrargyri* BerOc1.

In fumarate respiration, the pyruvate (electron donor) and the fumarate (electron acceptor) were all consumed at Tf in all the tested molybdate concentrations (Table 1). The concentration of succinate (from fumarate reduction) and acetate (from pyruvate oxidation), corresponding to the metabolites generated during fumarate respiration were produced as expected (Tf ranging from 30 to 40 mM), since one mole of fumarate (when it is reduced to succinate) accepts two electrons from one mole of pyruvate (Table 1). Low sulfide concentrations were also measured in fumarate respiration and were due to the initial addition of Na_2S as sulfur source in the culture medium (Fig. 3).

In sulfate respiration, the electron donor and acceptor when using lactate (electron donor) and sulfate (producing APS and bisulfite as electron acceptors) were partially consumed at Tf in the tested conditions, probably due to a surplus of substrates compared to fumarate respiration. Acetate (from lactate oxidation) and sulfides (from sulfate reduction), corresponding to the metabolites produced in this condition, were produced at concentrations range of

20-25 mM for acetate and 11-14 mM for sulfide in all the molybdate conditions, in accordance with the metabolism tested (Table 1, Fig. 3). When pyruvate and sulfate are used in sulfate respiration, pyruvate is totally consumed, producing the expected amount of acetate (ranging from 30 to 40 mM) and less sulfides (ranging from 5 to 8 mM) are produced (Table 1, Fig. 3), compared to the presence of lactate and sulfate. Two molecules of lactate are needed to reduce one molecule of sulfate in sulfate respiration, whereas four molecules of pyruvate are needed for this reduction (Keller and Wall, 2011). This explains the higher consumption of the electron donor (pyruvate) and the lower production of sulfides when using pyruvate and sulfate compared to those when using lactate and sulfate.

Molybdate altered the expression level of hgcA *and* sat *genes of* P. hydrargyri *BerOc1*

The expression level of *hgcA* gene involved in Hg methylation (Parks et al., 2013) and *sat*/*ycaO* genes involved in molybdate-sensitivity (Zane et al., 2020) were monitored (Fig. 4) in *P. hydrargyri* BerOc1 culture exposed to different molybdate concentrations.

Interestingly, the *hgcA* gene exhibited higher expression value ($p < 0.05$, Kruskal-Wallis test) when exposed to 0.1 mM of molybdate during fumarate respiration, as well as during sulfate respiration when lactate was used as the electron donor (Fig. 4A). No significant variations in *hgcA* fold change were observed during sulfate respiration when pyruvate was used ($p > 0.05$, Kruskal-Wallis test), despite molybdate's inhibition of Hg methylation under this condition (Fig. 2). This suggests once again that the cellular response to molybdate in Hg methylator organisms like *P. hydrargyri* BerOc1 is variable and dependent on cellular metabolism.

The *sat* gene is expressed in *P. hydrargyri* BerOc1 under all the tested conditions, including fumarate respiration (Fig. S1). When the cells were grown in fumarate respiration, no significant fold change was observed in the *sat* gene expression in the presence of molybdate ($p > 0.05$, Kruskal-Wallis test). However, for both sulfate-reducing conditions, the expression of *sat* gene was inhibited by molybdate (Fig. 4B). The molybdate inhibition of *sat* gene increase with higher molybdate concentrations ($p < 0.05$, Kruskal-Wallis test, when 0 mM is compared to 0.1 mM molybdate conditions). For *ycaO* gene expression (Fig. 4C), molybdate did not change the expression level of this gene ($p > 0.05$, Kruskal-Wallis test) in any of the tested metabolic conditions.

Discussion

In this study, we investigated the effect of molybdate on bacterial growth and Hg methylation using a SRB model (*P. hydrargyri* BerOc1) and a non-SRB model (*G. sulfurreducens* PCA). The results showed that molybdate inhibits the growth of the Hg methylating SRB *P. hydrargyri* BerOc1, regardless of the metabolic growth

conditions. While it is generally acknowledged that molybdate inhibits the sulfate metabolism of SRB (Biswas et al., 2009; Newport and Nedwell, 1988; Zane et al., 2020), molybdate inhibition of pyruvate fermentation in *D. vulgaris* Hildenborough have been previously reported (Zane et al., 2020, p. 2). Additionally, molybdate inhibits the growth of *Desulfovibrio desulfuricans* on sulfate-free lactate medium, when in co-culture with a methanogen (Pak K.-R. and Bartha R., 1998). Here, we demonstrated for the first time that molybdate inhibits the growth of *P. hydrargyri* BerOc1 during fumarate respiration, further indicating that molybdate inhibition is not specific to sulfate respiration. Molybdate inhibition of SRB involves Sat and YcaO-like proteins (Zane et al., 2020). As describes earlier, these proteins are likely involved in the formation of an unstable APS analogue in the presence of molybdate, leading to a non-productive ATP cycling. In this work, we showed that the expression of *sat* gene is constitutive in all the tested conditions, including fumarate respiration. Sat enzyme is involved in the activation of sulfate in both sulfate dissimilatory and assimilatory pathways (Abdulina et al., 2020) and may explain the constitutive expression of the *sat* gene even in non-sulfidogenic growth condition. If the Sat protein is active during fumarate respiration, the APS analog can still be formed, potentially leading to non-productive ATP cycling, and induce molybdate inhibition in this growth condition as well.

Interestingly, the sensitivity to molybdate was higher in fumarate respiration (complete inhibition at 1 mM) than in sulfate respiration (complete inhibition at 2 mM). It is known that molybdate in a sulfide-rich environment (i.e. sulfate respiration) may form molybdenite [$MoS_{2(s)}$] compounds which appear to occur in the periplasm and accumulate extracellularly or at the cell surface (Biswas et al., 2009; Tucker et al., 1997). This molybdate speciation could limit molybdate bioavailability and reduce the molybdate inhibitory effect during sulfidogenic growth conditions. Furthermore, when monitoring the expression of *sat* and *ycaO* genes involved in molybdate sensitivity (Zane et al., 2020), we observed that the expression of *sat* gene was inhibited at 0.1 mM in both sulfate-reducing conditions. However, its expression remained unchanged during fumarate respiration. The inhibition of *sat* gene during sulfidogenic growth conditions may reduce the inhibitory effect of molybdate on the growth of *P. hydrargyri* BerOc1 by mitigating the effect of the ATP 'futile' cycle.

Remarkably, the data presented in this work showed that molybdate inhibits Hg methylation process in *P. hydrargyri* BerOc1, even at concentrations where growth is not fully inhibited. The metallic ions zinc and cadmium (Schaefer et al., 2014) as well as copper at high concentrations (Lu et al., 2018) were shown to inhibit Hg methylation. In the case of the zinc inhibition, it was suggested that Hg uptake might occurs via an active zinc transporter leading to a competition for uptake between the two metals (Schaefer et al., 2014). A similar competition between the uptake of molybdate and Hg may occur. However, the competition between Hg and other

metal uptakes has been proposed for a decade but never been demonstrated. An alternative mechanism involving cellular ATP content could be also considered. Indeed, the Hg methylation process is energy-dependent (Schaefer et al., 2011) and the generation of an ATP 'futile' cycle via molybdate may harm the production of MeHg. In this study, we observed a higher inhibition of mercury methylation induced by molybdate when using pyruvate as an electron donor (complete inhibition at 0.1 mM of molybdate) compared to lactate (complete inhibition at 2 mM of molybdate). This disparity could be attributed to the difference in energy produced when using lactate versus pyruvate. While the oxidation of lactate coupled with sulfate reduction seems to generate low ATP via substrate phosphorylation (Peck, 1960), lactate metabolism leads to hydrogen production through hydrogenase activity (Berg et al., 1991), likely compensating for the lower energy yield. An overproduction of the [Ni-Fe] hydrogenase 1 was observed also under molybdate-stressed condition in *Desulfovibrio alaskensis* G20 (Nair et al., 2015). Consequently, under molybdate stress, sulfate respiration with lactate could be energetically more favorable for cell growth due to the enhanced hydrogenase activity. This could potentially reduce the inhibitory effect of molybdate on MeHg production when using lactate as electron donor under sulfidogenic growth conditions.

In ecological studies, the observed decrease of Hg methylation after addition of molybdate (Bouchet et al., 2018) is probably a result of molybdate-induced inhibition of this process in SRBs, regardless of whether they are under sulfidogenic or non-sulfidogenic metabolisms. Indeed, the inhibition of Hg methylation by molybdate observed in our study aligns with the findings in biofilms and periphyton from the Lake Titicaca hydrosystem (Bouchet et al., 2018). Despite the fact that sulfate reducers remain active in the presence of molybdate, Hg methylation in Lake Titicaca was inhibited, providing further support that molybdate inhibits this process in sulfate reducers.

The data presented in this work also showed that the inhibition of Hg methylation in the presence of molybdate is not linked to an inhibition of *hgcA* gene expression (involved in Hg methylation (Parks et al., 2013)). *hgcA* expression was on the contrary higher when Hg methylation is completely inhibited during fumarate respiration and sulfate respiration when using lactate as electron donor. Although the link between *hgcA* expression and MeHg production was not demonstrated before (Goñi-Urriza et al., 2015), the increase seen in the expression of *hgcA* could be a cellular response to overcome the decrease seen in the Hg methylation rate in the presence of molybdate. Indeed, the decrease in MeHg production may increase the concentration of Hg(II) in the cell. This overexpression of *hgcA* could potentially serve to increase the rate of Hg methylation as a mechanism of resistance against the toxicity associated with Hg(II). *arsR* gene of the ArsR/SmtB family of metal-sensory transcriptional regulators (Saha et al., 2017), is found upstream *hgcAB* in multiple Hg methylating SRB (Goñi-Urriza et al., 2020) and is

responsive to arsenic and homocysteine (Gionfriddo et al., 2022). It will be interesting to investigate in future studies the role of ArsR in *hgcAB* regulation in respect to molybdate and its inhibitory effect.

As expected molybdate does not inhibits the growth of the iron-reducing and the Hg methylating bacterium *G. sulfurreducens* PCA in fumarate respiration. This resistance might be due to the absence of *sat* and *ycaO* genes, involved in molybdate sensitivity (Zane et al., 2020) in the genome of *G. sulfurreducens* PCA. Additionally, molybdate does not inhibit the Hg methylation process of *G. sulfurreducens* PCA. Ecological studies indicate that molybdate only partially inhibits the Hg methylation activity of certain anoxic sediments. It has been suggested that iron-reducing bacteria, like *G. sulfurreducens* PCA, might contribute to this 'molybdate-independent' methylation process (Fleming et al., 2006). This is consistent with our findings, where we observed no inhibition of growth or Hg methylation activity with a pure culture of *G. sulfurreducens* PCA.

Conclusions

Overall, this study demonstrates that molybdate inhibits the growth of *P. hydrargyri* BerOc1 during both sulfate and fumarate respiration, with a higher level of inhibition observed during fumarate respiration. Even more interesting, molybdate was shown to inhibit mercury methylation in *P. hydrargyri* BerOc1. This inhibition may be linked to cellular energy production, which is inherently metabolism-dependent. The data presented in this work highlight the importance of studying molybdate-induced inhibition in regards to *sat* coupled to *hgcA* and Hg methylation in order to advance our knowledge regarding the players involved in MeHg production at the environmental level.

Acknowledgments

We thank Marion Guignard for her guidance on the ion chromatography technique.

References

Abdulina, D., Kováč, J., Iutynska, G., Kushkevych, I., 2020. ATP sulfurylase activity of sulfate-reducing bacteria from various ecotopes. 3 Biotech 10, 55. https://doi.org/10.1007/s13205-019-2041-9

Bakour, I., Isaure, M.-P., Barrouilhet, S., Goñi-Urriza, M., Monperrus, M., 2023. Coupling fluorescent probes to characterize S-containing compounds in a sulfate reducing bacteria involved in Hg methylation. Talanta Open 7, 100228. https://doi.org/10.1016/j.talo.2023.100228

Barrouilhet, S., Monperrus, M., Tessier, E., Khalfaoui-Hassani, B., Guyoneaud, R., Isaure, M.-P., Goñi-Urriza, M., 2022. Effect of exogenous and endogenous sulfide on the production and the export of methylmercury by sulfate-reducing bacteria. Environ. Sci. Pollut. Res. https://doi.org/10.1007/s11356-022-22173-y

Barton, L.L., Fauque, G.D., 2009. Chapter 2 Biochemistry, Physiology and Biotechnology of Sulfate-Reducing Bacteria, in: Advances in Applied Microbiology. Academic Press, pp. 41–98. https://doi.org/10.1016/S0065-2164(09)01202-7

Benoit J. M., Gilmour C. C., Mason R. P., 2001. Aspects of Bioavailability of Mercury for Methylation in Pure Cultures of Desulfobulbus propionicus (1pr3). Appl. Environ. Microbiol. 67, 51–58. https://doi.org/10.1128/AEM.67.1.51-58.2001

Benoit, J.M., Gilmour, C.C., Mason, R.P., 2001. Aspects of Bioavailability of Mercury for Methylation in Pure Cultures of *Desulfobulbus propionicus* (1pr3). Appl. Environ. Microbiol. 67, 51–58. https://doi.org/10.1128/AEM.67.1.51-58.2001

Berg, W.A. van den, Dongen, W.M. van, Veeger, C., 1991. Reduction of the amount of periplasmic hydrogenase in Desulfovibrio vulgaris (Hildenborough) with antisense RNA: direct evidence for an important role of this hydrogenase in lactate metabolism. J. Bacteriol. 173, 3688–3694. https://doi.org/10.1128/jb.173.12.3688-3694.1991

Biswas, K.C., Woodards, N.A., Xu, H., Barton, L.L., 2009. Reduction of molybdate by sulfate-reducing bacteria. BioMetals 22, 131–139. https://doi.org/10.1007/s10534-008-9198-8

Bouchet, S., Goñi-Urriza, M., Monperrus, M., Guyoneaud, R., Fernandez, P., Heredia, C., Tessier, E., Gassie, C., Point, D., Guédron, S., Achá, D., Amouroux, D., 2018. Linking Microbial Activities and Low-Molecular-Weight Thiols to Hg Methylation in Biofilms and Periphyton from High-Altitude Tropical Lakes in the Bolivian Altiplano. Environ. Sci. Technol. 52, 9758–9767. https://doi.org/10.1021/acs.est.8b01885

Bravo, A.G., Peura, S., Buck, M., Ahmed, O., Mateos-Rivera, A., Herrero Ortega, S., Schaefer, J.K., Bouchet, S., Tolu, J., Björn, E., Bertilsson, S., 2018. Methanogens and Iron-Reducing Bacteria: the Overlooked Members of Mercury-Methylating Microbial Communities in Boreal Lakes. Appl. Environ. Microbiol. 84, e01774-18. https://doi.org/10.1128/AEM.01774-18

Caccavo F, Lonergan D J, Lovley D R, Davis M, Stolz J F, McInerney M J, 1994. Geobacter sulfurreducens sp. nov., a hydrogen- and acetate-oxidizing dissimilatory metal-reducing microorganism. Appl. Environ. Microbiol. 60, 3752–3759. https://doi.org/10.1128/aem.60.10.3752-3759.1994

Carlson, H.K., Youngblut, M.D., Redford, S.A., Williamson, A.J., Coates, J.D., 2021. Sulfate adenylyl transferase kinetics and mechanisms of metabolic inhibitors of microbial sulfate respiration. ISME Commun. 1, 67. https://doi.org/10.1038/s43705-021-00069-1

Chen, C., Amirbahman, A., Fisher, N., Harding, G., Lamborg, C., Nacci, D., Taylor, D., 2008. Methylmercury in Marine Ecosystems: Spatial Patterns and Processes of Production, Bioaccumulation, and Biomagnification. EcoHealth 5, 399–408. https://doi.org/10.1007/s10393-008-0201-1

CLINE, J.D., 1969. SPECTROPHOTOMETRIC DETERMINATION OF HYDROGEN SULFIDE IN NATURAL WATERS1. Limnol. Oceanogr. 14, 454–458. https://doi.org/10.4319/lo.1969.14.3.0454

Compeau, G.C., Bartha, R., 1985. Sulfate-Reducing Bacteria: Principal Methylators of Mercury in Anoxic Estuarine Sediment. Appl. Environ. Microbiol. 50, 498.

Compeau Geoffrey C., Bartha Richard, 1987. Effect of Salinity on Mercury-Methylating Activity of Sulfate-Reducing Bacteria in Estuarine Sediments. Appl. Environ. Microbiol. 53, 261–265. https://doi.org/10.1128/aem.53.2.261-265.1987

Cooper, C.J., Zheng, K., Rush, K.W., Johs, A., Sanders, B.C., Pavlopoulos, G.A., Kyrpides, N.C., Podar, M., Ovchinnikov, S., Ragsdale, S.W., Parks, J.M., 2020. Structure determination of the HgcAB complex using metagenome sequence data: insights into microbial mercury methylation. Commun. Biol. 3, 320. https://doi.org/10.1038/s42003-020-1047-5

Cypionka, H., 1989. Characterization of sulfate transport in Desulfovibrio desulfuricans. Arch. Microbiol. 152, 237–243. https://doi.org/10.1007/BF00409657

Ferreira, D., Barbosa, A.C.C., Oliveira, G.P., Catarino, T., Venceslau, S.S., Pereira, I.A.C., 2022. The DsrD functional marker protein is an allosteric activator of the DsrAB dissimilatory sulfite reductase. Proc. Natl. Acad. Sci. 119, e2118880119. https://doi.org/10.1073/pnas.2118880119

Fleming, E.J., Mack, E.E., Green, P.G., Nelson, D.C., 2006. Mercury Methylation from Unexpected Sources: Molybdate-Inhibited Freshwater Sediments and an Iron-Reducing Bacterium. Appl. Environ. Microbiol. 72, 457–464. https://doi.org/10.1128/AEM.72.1.457-464.2006

Gentès, S., Monperrus, M., Legeay, A., Maury-Brachet, R., Davail, S., André, J.-M., Guyoneaud, R., 2013. Incidence of invasive macrophytes on methylmercury budget in temperate lakes: Central role of bacterial periphytic communities. Environ. Pollut. 172, 116–123. https://doi.org/10.1016/j.envpol.2012.08.004

Gilmour, C.C., Bullock, A.L., McBurney, A., Podar, M., Elias, D.A., 2018. Robust Mercury Methylation across Diverse Methanogenic Archaea. mBio 9. https://doi.org/10.1128/mBio.02403-17

Gilmour, C.C., Henry, E.A., 1991. Mercury methylation in aquatic systems affected by acid deposition. Environ. Pollut. Barking Essex 1987 71, 131–169. https://doi.org/10.1016/0269-7491(91)90031-q

Gilmour, C.C., Henry, E.A., Mitchell, R., 1992. Sulfate stimulation of mercury methylation in freshwater sediments. Environ. Sci. Technol. 26, 2281–2287. https://doi.org/10.1021/es00035a029

Gionfriddo, C.M., Soren, A.B., Wymore, A., Hartnett, D.S., Podar, M., Parks, J.M., Elias, D.A., Gilmour, C.C., 2022. Transcriptional control of hgcAB by an ArsR-like regulator in Pseudodesulfovibrio mercurii ND132. bioRxiv. https://doi.org/10.1101/2022.10.17.512643

Goñi-Urriza, M., Corsellis, Y., Lanceleur, L., Tessier, E., Gury, J., Monperrus, M., Guyoneaud, R., 2015. Relationships between bacterial energetic metabolism, mercury methylation potential, and hgcA/hgcB gene expression in Desulfovibrio dechloroacetivorans BerOc1. Environ. Sci. Pollut. Res. 22, 13764–13771. https://doi.org/10.1007/s11356-015-4273-5

Goñi-Urriza, M., Klopp, C., Ranchou-Peyruse, M., Ranchou-Peyruse, A., Monperrus, M., Khalfaoui-Hassani, B., Guyoneaud, R., 2020. Genome insights of mercury methylation among Desulfovibrio and Pseudodesulfovibrio strains. Microorg. Met. Interact. 171, 3–12. https://doi.org/10.1016/j.resmic.2019.10.003

Hines, M.E., Poitras, E.N., Covelli, S., Faganeli, J., Emili, A., Žižek, S., Horvat, M., 2012. Mercury methylation and demethylation in Hg-contaminated lagoon sediments (Marano and Grado Lagoon, Italy). Estuar. Coast. Shelf Sci. 113, 85–95. https://doi.org/10.1016/j.ecss.2011.12.021

Hong Young-Seoub, Kim Yu-Mi, Lee Kyung-Eun, 2012. Methylmercury Exposure and Health Effects. J Prev Med Public Health 45, 353–363. https://doi.org/10.3961/jpmph.2012.45.6.353

Isaure, M.-P., Albertelli, M., Kieffer, I., Tucoulou, R., Petrel, M., Gontier, E., Tessier, E., Monperrus, M., Goñi-Urriza, M., 2020. Relationship Between Hg Speciation and Hg Methylation/Demethylation Processes in the Sulfate-Reducing Bacterium Pseudodesulfovibrio hydrargyri: Evidences From HERFD-XANES and Nano-XRF. Front. Microbiol. 11, 2506. https://doi.org/10.3389/fmicb.2020.584715

Keller, K.L., Wall, J.D., 2011. Genetics and molecular biology of the electron flow for sulfate respiration in desulfovibrio. Front. Microbiol. 2, 135–135. https://doi.org/10.3389/fmicb.2011.00135

King, J.K., Kostka, J.E., Frischer, M.E., Saunders, F.M., 2000. Sulfate-Reducing Bacteria Methylate Mercury at Variable Rates in Pure Culture and in Marine Sediments. Appl. Environ. Microbiol. 66, 2430–2437. https://doi.org/10.1128/AEM.66.6.2430-2437.2000

Kleikemper, J., Pelz, O., Schroth, M.H., Zeyer, J., 2002. Sulfate-reducing bacterial community response to carbon source amendments in contaminated aquifer microcosms. FEMS Microbiol. Ecol. 42, 109–118. https://doi.org/10.1111/j.1574-6941.2002.tb01000.x

Lee, J., Burow, L., Woebken, D., Everroad, R., Kubo, M., Spormann, A., Weber, P., Pett-Ridge, J., Bebout, B., Hoehler, T., 2014. Fermentation couples Chloroflexi and sulfate-reducing bacteria to Cyanobacteria in hypersaline microbial mats. Front. Microbiol. 5. https://doi.org/10.3389/fmicb.2014.00061

491 Lin, H., Morrell-Falvey, J.L., Rao, B., Liang, L., Gu, B., 2014. Coupled Mercury–Cell Sorption, Reduction,
492 and Oxidation on Methylmercury Production by Geobacter sulfurreducens PCA. Environ. Sci.
493 Technol. 48, 11969–11976. https://doi.org/10.1021/es502537a
494 Lu, X., Johs, A., Zhao, L., Wang, L., Pierce, E.M., Gu, B., 2018. Nanomolar Copper Enhances Mercury
495 Methylation by Desulfovibrio desulfuricans ND132. Environ. Sci. Technol. Lett. 5, 372–376.
496 https://doi.org/10.1021/acs.estlett.8b00232
497 Ma, M., Du, H., Wang, D., 2019. Mercury methylation by anaerobic microorganisms: A review. Crit.
498 Rev. Environ. Sci. Technol. 49, 1893–1936. https://doi.org/10.1080/10643389.2019.1594517
499 Meyer, B., Kuever, J., 2008. Homology Modeling of Dissimilatory APS Reductases (AprBA) of Sulfur-
500 Oxidizing and Sulfate-Reducing Prokaryotes. PLOS ONE 3, e1514.
501 https://doi.org/10.1371/journal.pone.0001514
502 Monperrus, M., Rodriguez Gonzalez, P., Amouroux, D., Garcia Alonso, J.I., Donard, O.F.X., 2008.
503 Evaluating the potential and limitations of double-spiking species-specific isotope dilution
504 analysis for the accurate quantification of mercury species in different environmental
505 matrices. Anal. Bioanal. Chem. 390, 655–666. https://doi.org/10.1007/s00216-007-1598-z
506 Nair, R.R., Silveira, C.M., Diniz, M.S., Almeida, M.G., Moura, J.J.G., Rivas, M.G., 2015. Changes in
507 metabolic pathways of Desulfovibrio alaskensis G20 cells induced by molybdate excess. JBIC
508 J. Biol. Inorg. Chem. 20, 311–322. https://doi.org/10.1007/s00775-014-1224-4
509 Newport, P.J., Nedwell, D.B., 1988. The mechanisms of inhibition of Desulfovibrio and
510 Desulfotomaculum species by selenate and molybdate. J. Appl. Bacteriol. 65, 419–423.
511 https://doi.org/10.1111/j.1365-2672.1988.tb01911.x
512 Oliveira, T.F., Vonrhein, C., Matias, P.M., Venceslau, S.S., Pereira, I.A.C., Archer, M., 2008. The Crystal
513 Structure of Desulfovibrio vulgaris Dissimilatory Sulfite Reductase Bound to DsrC Provides
514 Novel Insights into the Mechanism of Sulfate Respiration*. J. Biol. Chem. 283, 34141–34149.
515 https://doi.org/10.1074/jbc.M805643200
516 Overmann, J., Fischer, U., Pfennig, N., 1992. A new purple sulfur bacterium from saline littoral
517 sediments, Thiorhodovibrio winogradskyi gen. nov. and sp. nov. Arch. Microbiol. 157, 329–
518 335. https://doi.org/10.1007/BF00248677
519 Pak K.-R., Bartha R., 1998. Mercury Methylation by Interspecies Hydrogen and Acetate Transfer
520 between Sulfidogens and Methanogens. Appl. Environ. Microbiol. 64, 1987–1990.
521 https://doi.org/10.1128/AEM.64.6.1987-1990.1998
522 Parks, J.M., Johs, A., Podar, M., Bridou, R., Hurt, R.A., Smith, S.D., Tomanicek, S.J., Qian, Y., Brown,
523 S.D., Brandt, C.C., Palumbo, A.V., Smith, J.C., Wall, J.D., Elias, D.A., Liang, L., 2013. The
524 Genetic Basis for Bacterial Mercury Methylation. Science 339, 1332.
525 https://doi.org/10.1126/science.1230667
526 Peck, H.D., 1960. Evidence for Oxidative Phosphorylation during the Reduction of Sulfate with
527 Hydrogen by Desulfovibrio desulfuricans. J. Biol. Chem. 235, 2734–2738.
528 https://doi.org/10.1016/S0021-9258(19)76945-2
529 Pfennig, N., Trüper, H.G., 1992. The Family Chromatiaceae, in: Balows, A., Trüper, H.G., Dworkin, M.,
530 Harder, W., Schleifer, K.-H. (Eds.), The Prokaryotes: A Handbook on the Biology of Bacteria:
531 Ecophysiology, Isolation, Identification, Applications. Springer New York, New York, NY, pp.
532 3200–3221. https://doi.org/10.1007/978-1-4757-2191-1_8
533 Podar, M., Gilmour, C.C., Brandt, C.C., Soren, A., Brown, S.D., Crable, B.R., Palumbo, A.V.,
534 Somenahally, A.C., Elias, D.A., 2015. Global prevalence and distribution of genes and
535 microorganisms involved in mercury methylation. Sci. Adv. 1, e1500675–e1500675.
536 https://doi.org/10.1126/sciadv.1500675
537 Ranchou-Peyruse, M., Goñi-Urriza, M., Guignard, M., Goas, M., Ranchou-Peyruse, A., Guyoneaud, R.,
538 2018. Pseudodesulfovibrio hydrargyri sp. nov., a mercury-methylating bacterium isolated
539 from a brackish sediment. Int. J. Syst. Evol. Microbiol. 68, 1461–1466.
540 Ranchou-Peyruse, M., Monperrus, M., Bridou, R., Duran, R., Amouroux, D., Salvado, J.C., Guyoneaud,
541 R., 2009. Overview of Mercury Methylation Capacities among Anaerobic Bacteria Including

Representatives of the Sulphate-Reducers: Implications for Environmental Studies. Geomicrobiol. J. 26, 1–8. https://doi.org/10.1080/01490450802599227
Saha, R.P., Samanta, S., Patra, S., Sarkar, D., Saha, A., Singh, M.K., 2017. Metal homeostasis in bacteria: the role of ArsR–SmtB family of transcriptional repressors in combating varying metal concentrations in the environment. BioMetals 30, 459–503. https://doi.org/10.1007/s10534-017-0020-3
Schaefer, J.K., Rocks, S.S., Zheng, W., Liang, L., Gu, B., Morel, F.M.M., 2011. Active transport, substrate specificity, and methylation of Hg(II) in anaerobic bacteria. Proc. Natl. Acad. Sci. 108, 8714. https://doi.org/10.1073/pnas.1105781108
Schaefer, J.K., Szczuka, A., Morel, F.M.M., 2014. Effect of Divalent Metals on Hg(II) Uptake and Methylation by Bacteria. Environ. Sci. Technol. 48, 3007–3013. https://doi.org/10.1021/es405215v
Smith, S.D., Bridou, R., Johs, A., Parks, J.M., Elias, D.A., Hurt, R.A., Brown, S.D., Podar, M., Wall, J.D., 2015. Site-Directed Mutagenesis of HgcA and HgcB Reveals Amino Acid Residues Important for Mercury Methylation. Appl. Environ. Microbiol. 81, 3205. https://doi.org/10.1128/AEM.00217-15
Taylor, B.F., Oremland, R.S., 1979. Depletion of adenosine triphosphate inDesulfovibrio by oxyanions of group VI elements. Curr. Microbiol. 3, 101–103. https://doi.org/10.1007/BF02602440
Tucker, M.D., Barton, L.L., Thomson, B.M., 1997. Reduction and Immobilization of Molybdenum by Desulfovibrio desulfuricans. J. Environ. Qual. 26, 1146–1152. https://doi.org/10.2134/jeq1997.00472425002600040029x
Vigneron, A., Cruaud, P., Aubé, J., Guyoneaud, R., Goñi-Urriza, M., 2021. Transcriptomic evidence for versatile metabolic activities of mercury cycling microorganisms in brackish microbial mats. Npj Biofilms Microbiomes 7, 83. https://doi.org/10.1038/s41522-021-00255-y
Villar, E., Cabrol, L., Heimbürger-Boavida, L.-E., 2020. Widespread microbial mercury methylation genes in the global ocean. Environ. Microbiol. Rep. 12, 277–287. https://doi.org/10.1111/1758-2229.12829
Wang, Y., Robison, T., Wiatrowski, H., 2013. The impact of ionic mercury on antioxidant defenses in two mercury-sensitive anaerobic bacteria. BioMetals 26, 1023–1031. https://doi.org/10.1007/s10534-013-9679-2
Zane, G.M., Wall, J.D., De León, K.B., 2020. Novel Mode of Molybdate Inhibition of Desulfovibrio vulgaris Hildenborough. Front. Microbiol. 11. https://doi.org/10.3389/fmicb.2020.610455

Funding statement

This work was supported by the French National Research Agency [ANR MICROMER ANR-21-CE34-0014] and by the Excellence Initiative of Université de Pau et des Pays de l'Adour – I-Site E2S UPPA [Hub MeSMic], a French "Investissements d'Avenir" program.

Competing Interests

The authors have no relevant financial or non-financial interests to disclose.

Author Contributions

RG, DS, BKH and MSGU conceptualized the work, designed experiments and analyzed the data. DS performed experiments. ET, CG and MRP helped setting up experiments and data analysis of GC-ICP-MS, qRT-PCR and

ion chromatography, respectively. DS and BKH wrote the manuscript and RG and MSGU helped achieving the final draft of the manuscript. All authors participated in the critical thinking of the data and edited the manuscript.

Ethics approval

Not applicable. This study does not involve human participants.

Consent to participate

Not applicable.

Consent to publish

Not applicable.

Figure and table legends

Figure 1: Effect of molybdate on the growth of *P. hydrargyri* BerOc1 and *G. sulfurreducens* PCA. *P. hydrargyri* BerOc1 was grown on sulfate respiration with sulfate and lactate (black triangle), sulfate and pyruvate (black square) or on fumarate respiration with fumarate and pyruvate (black circle) as substrates. *G. sulfurreducens* PCA was grown on fumarate respiration in presence of acetate and fumarate (white square). For each condition, strains were grown in presence of increasing molybdate concentrations (0, 0.01, 0.05, 0.1, 1 and 2 mM) and 0.05 µM of Hg(II). The biomass production is reported in percentage while 100% of biomass production corresponds to the biomass production of strains in the condition with no molybdate. The inset shows the % of biomass production values at 0, 0.01, 0.005 and 0.1 mM of molybdate. Experiments were performed in triplicate.

Figure 2: Effect of molybdate on Hg(II) methylation in *P. hydrargyri* BerOc1 and *G. sulfurreducens* PCA. MeHg production is expressed in ng/cell of *P. hydrargyri* BerOc1 grown with sulfate and lactate (black triangle), sulfate and pyruvate (black square) or fumarate and pyruvate (black circle) as substrates. *G. sulfurreducens* PCA was grown in presence of acetate and fumarate (white square). For each condition, strains were grown in presence of increasing molybdate concentrations (0, 0.01, 0.05, 1 and 2 mM) and 0.05 µM of Hg(II). The inset shows the % of MeHg production values at 0, 0.01, 0.005 and 0.1 mM of molybdate. Experiments were performed in triplicate.

Figure 3: Sulfide's production in *P. hydrargyri* BerOc1 and *G. sulfurreducens* PCA. Sulfide production (mM) was measured at Tf in *P. hydrargyri* BerOc1 grown in sulfate (Suf/Lact and Sulf/Pyr) and fumarate respiration (Fum/Pyr) and in *G. sulfurreducens* PCA grown in fumarate respiration (Acet/Fum). Fum: fumarate, Pyr: pyruvate, Sulf: sulfate, Lact: lactate, Acet: acetate.

Figure 4: Expression of genes involved in Hg methylation (*hgcA*) and molybdate sensitivity (*sat* and *ycaO*) in *P. hydrargyri* BerOc1. Real-time RT-PCR was performed on cultures of *P. hydrargyri* BerOc1 grown on sulfate respiration with lactate (Sulf/Lact) or pyruvate (Sulf/Pyr) as electron donor, as well as on fumarate respiration with pyruvate (Fum/Pyr). The expression level of *hgcA* (A), *sat* (B) and *ycaO* (C) genes were monitored, in the presence of increasing molybdate concentrations (0, 0.01, and 0.1 mM) and 0.05 µM of Hg(II). Data were normalized using *gyrB* gene expression as a housekeeping gene in the same condition, following double delta Ct method. Error bars represent the standard deviations of three independent replicates, each one measured three times.

Table 1: The growth parameters of *P. hydrargyri* BerOc1 (BerOc1) are presented in biomass production (ΔOD_{600}) and µ (h^{-1}). 40 mM of the substrates were added at the initial time of the experiment. The values of the electron acceptor and donor are reported in mM of the measured substrate at Tf. The metabolites produced from the electron acceptor and donor are reported in mM of the produced metabolites at Tf. Fum; fumarate, Pyr; pyruvate, Sulf; sulfate, Lact; lactate, Sulfi; sulfide, Acet; acetate, Succ; succinate, NA : not applicable, ND : not determined.

Supplementary Materials

Figure S1: Expression of *P. hydrargyri* BerOc1 *sat* gene at 0 mM of molybdate.

Table S1: Growth parameters of *G. sulfurreducens* PCA.

Table S2: Quantification of the Hg(II) methylation (MeHg production) and MeHg demethylation (Hg(II) production).

629 Figure 1

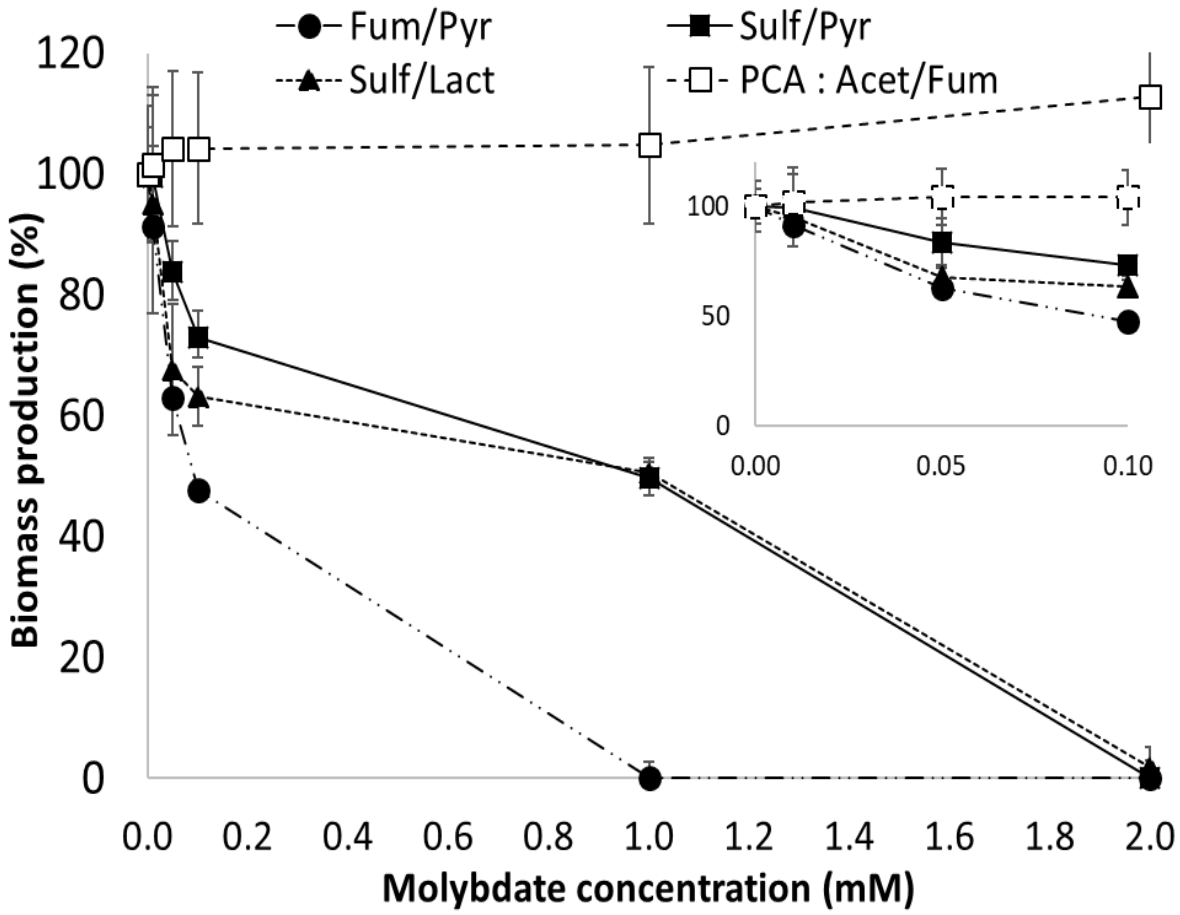

630

631

632 Figure 2

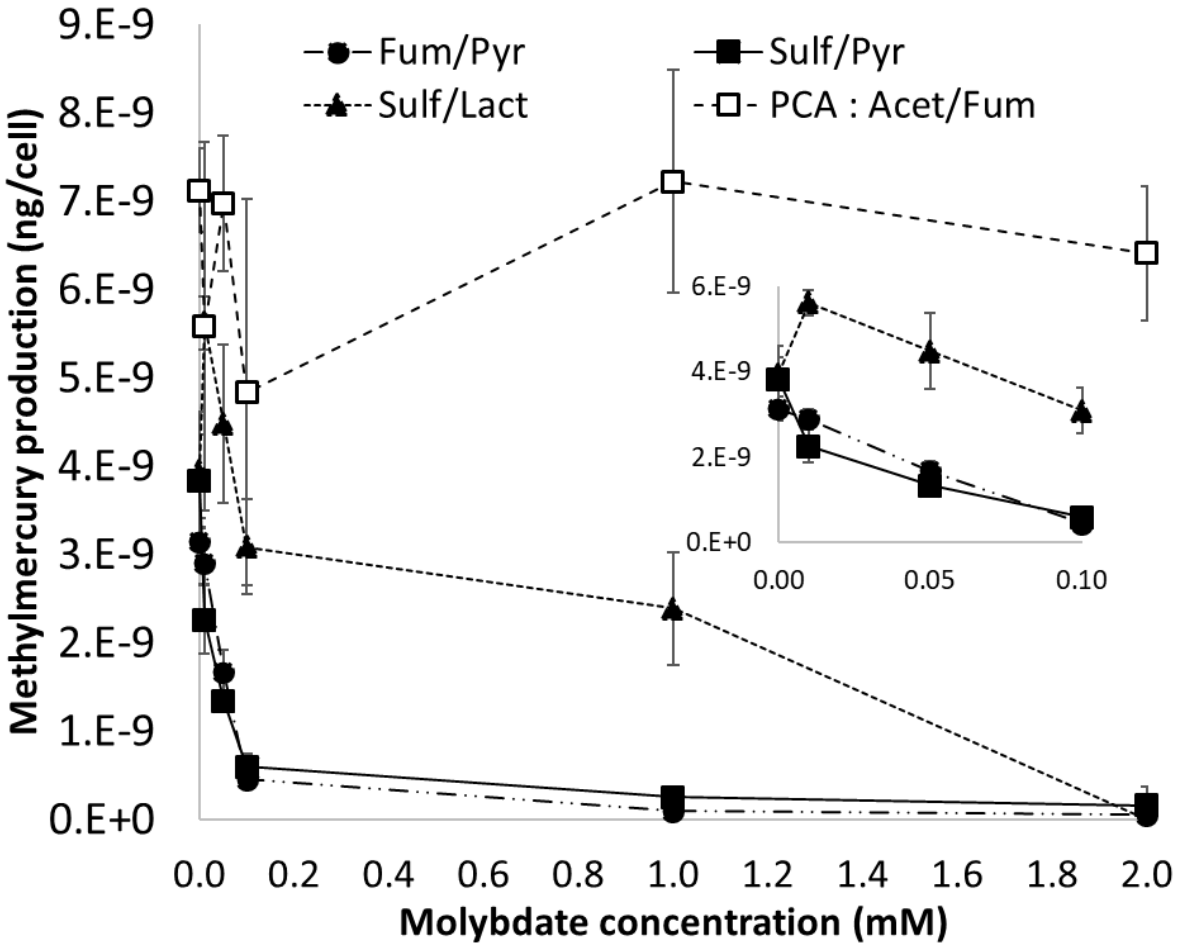

633

634

635

Figure 3

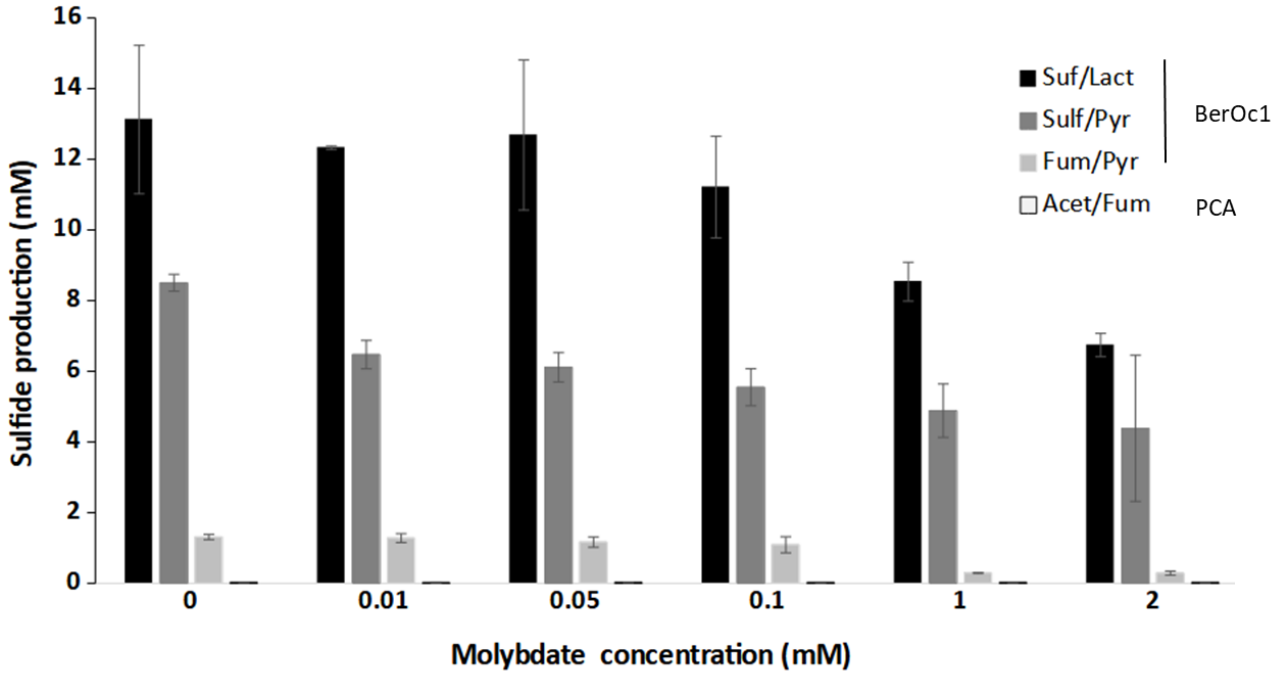
Sulfide production (mM)
16
14
12
10
8
6
4
2
0
0
0.01
0.05
0.1
1
2
Molybdate concentration (mM)
Suf/Lact
Sulf/Pyr
Fum/Pyr
Acet/Fum
BerOc1
PCA

651 Figure 4

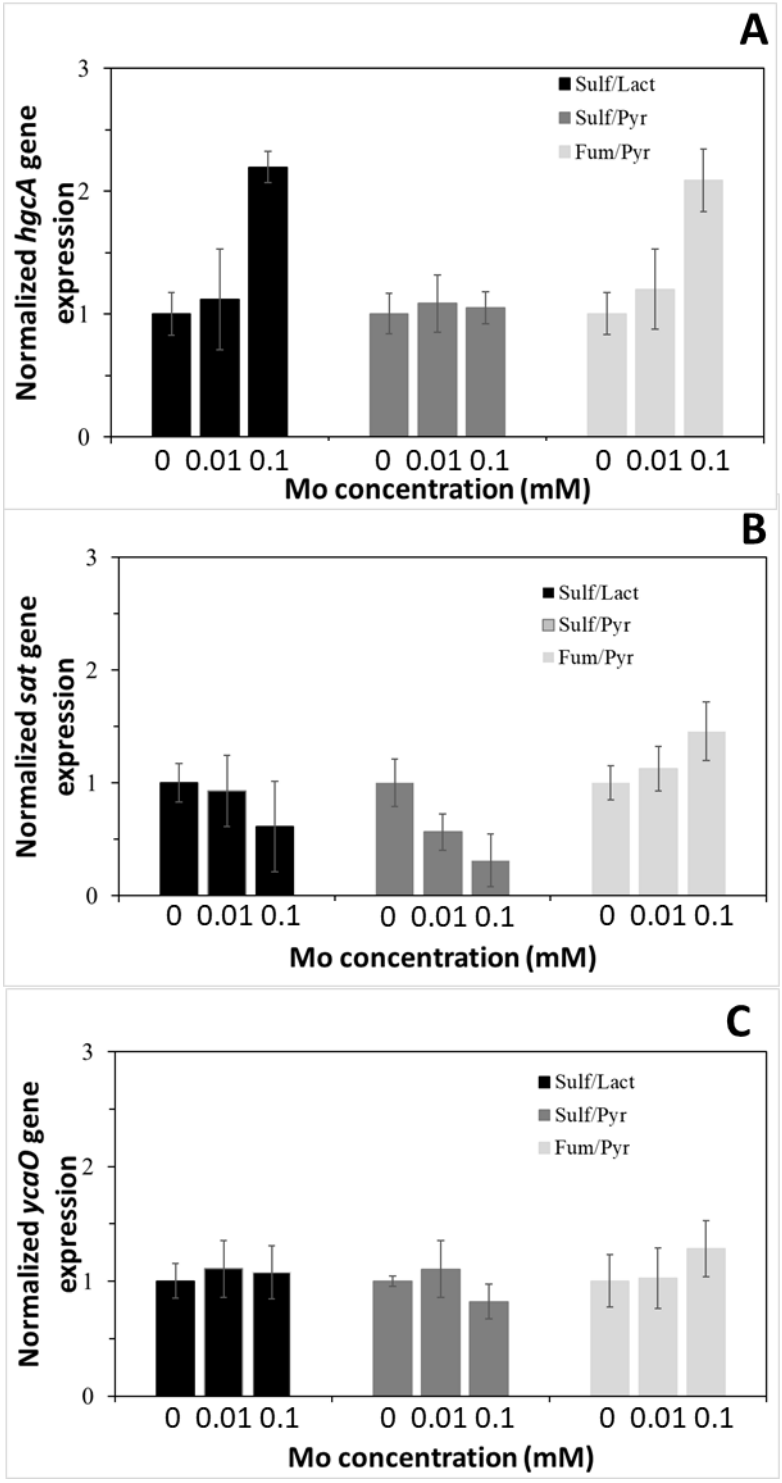

652

653

654

655

656 Table 1

		Growth parameters		Metabolite measurements			
	Mo (mM)	Biomass production (ΔOD_{600})	μ (h^{-1})	Electron donor mM at Tf	Electron acceptor mM at Tf	Metabolite produced from the electron donor (mM at Tf)	Metabolite produced from the electron acceptor (mM at Tf)
BerOc1 Fum/Pyr	0	0.23 ± 0.001	0.04 ± 0.001	Pyr : 0	Fum : 0	Acet : 41.80 ± 1.59	Succ : 34.62 ± 2.22
	0.01	0.21 ± 0.003	0.04 ± 0.002	Pyr : 0	Fum : 0	Acet : 39.27 ± 1.74	Succ : 35.94 ± 1.65
	0.05	0.15 ± 0.002	0.02 ± 0.001	ND	ND	ND	ND
	0.1	0.11 ± 0.003	0.02 ± 0.001	Pyr : 0	Fum : 0	Acet : 30.63 ± 1.86	Succ : 38.49 ± 0.82
	1	NG	NG	-	-	-	-
	2	NG	NG	-	-	-	-
BerOc1 Sulf/Pyr	0	0.16 ± 0.005	0.07 ± 0.002	Pyr : 0	sulf : 35.15 ± 4.93	Acet : 37.91 ± 1.29	Sulfi : 8.50 ± 0.24
	0.01	0.16 ± 0.003	0.06 ± 0.004	Pyr : 0	sulf : 36.16 ± 5.22	Acet : 31.92 ± 2.04	Sulfi : 6.47 ± 0.40
	0.05	0.13 ± 0.003	0.04 ± 0.002	ND	ND	ND	ND
	0.1	0.11 ± 0.003	0.03 ± 0.001	Pyr : 0	sulf : 36.34 ± 5.23	Acet : 32.78 ± 1.42	Sulfi : 5.55 ± 0.52
	1	0.08 ± 0.003	0.02 ± 0.001	ND	ND	ND	ND
	2	NG	NG	-	-	-	-
BerOc1 Sulf/Lact	0	0.09 ± 0.007	0.05 ± 0.001	Lact : 11.65 ± 0.22	Sulf : 29.73 ± 0.40	Acet : 23.00 ± 0.51	Sulfi : 13.12 ± 2.10
	0.01	0.08 ± 0.009	0.04 ± 0.003	Lact : 10.94 ± 0.58	Sulf : 30.15 ± 1.32	Acet : 24.88 ± 2.71	Sulfi : 12.33± 0.05
	0.05	0.06 ± 0.005	0.03 ± 0.004	ND	ND	ND	ND
	0.1	0.05 ± 0.006	0.03 ± 0.001	Lact : 14.85 ± 0.44	Sulf : 32.70 ± 0.36	Acet : 19.46 ± 0.96	Sulfi : 11.21 ± 1.44
	1	0.04 ± 0.002	0.02 ± 0.002	ND	ND	ND	ND
	2	NG	NG	-	-	-	-

657

658

659